Journal of Hydrology: Regional Studies 38 (2021) 100973

Contents lists available at ScienceDirect

Journal of Hydrology: Regional Studies

journal homepage: www.elsevier.com/locate/ejrh

# Exploring future vulnerabilities of subalpine Italian regulated lakes under different climate scenarios: bottom-up vs top-down and CMIP5 vs CMIP6

Francesca Casale [a,*], Flavia Fuso [a], Matteo Giuliani [b], Andrea Castelletti [b], Daniele Bocchiola [a]

[a] Department of Civil and Environmental Engineering, Politecnico di Milano, 20133 Milano Italy
[b] Department of Electronics, Information, and Bioengineering, Politecnico di Milano, 20133 Milano Italy

ARTICLE INFO

*Keywords:*
Hydro-climatic variability
Lake operation
Hydrological modelling
Climate change
Sixth Assessment Report

ABSTRACT

*Study region:* Lake Como watershed, between Northern Italy and Switzerland (Europe).
*Study focus:* We analyse the potential vulnerabilities of existing water management practice in sub-alpine regulated lakes. We comparatively explore a wide range of inflow scenarios using a bottom-up approach, relying on synthetic alteration of observed climate drivers, and a top-down procedure, working with both CMIP5 and CMIP6 projections. We then run an ANOVA to back-track components of variability in the projected lake inflows to key uncertainty sources.
*New hydrological insights for the region:* Results show a general worsening of lake management performance under the top-down projections with respect to the equivalent bottom-up scenarios, with the CMIP6 ensemble yielding worst conditions than CMIP5. Moreover, the top-down, physically-based scenarios highlight non-linear patterns of climatic/hydrological variability that challenge historical management, while bottom-up projections overlook these trends. The results of the ANOVA demonstrate that at mid-century the choice of the general circulation model is the dominant factor influencing the variability, while climate patterns become more relevant toward the end of the century. Overall, our study provides numerical evidence of the ongoing and projected impact of climate change on sub-alpine regions and outlines how different inflow scenarios generation approaches result in different inflow variability and associated risk assessment.

## 1. Introduction

Water from the Alps is paramount for sustaining many European rivers and lakes as it supports a variety of water-related activities. Alpine hydropower contributes about 13% of the Italian national production (Gaudard et al., 2014; GSE - Gestore Servizi Energetici, 2021). Water from the Alps mostly reaches the Po Valley, which is the most productive agricultural area of Europe, where farming areas cover 45% of the catchment (Bocchiola et al., 2013; Giuliani et al., 2016a), and contribute to 35% of Italian agricultural production (Zullo et al., 2019). Besides, the Po Valley hosts 21 M people and 48% of Italian industries (ibidem).

Recent fallout of climate change on the cryosphere-driven hydrology of the Alps is widely acknowledged (Bocchiola, 2014; Fatichi

* Corresponding author.
*E-mail address:* francesca.casale@polimi.it (F. Casale).

https://doi.org/10.1016/j.ejrh.2021.100973
Received 15 September 2021; Received in revised form 9 November 2021; Accepted 25 November 2021
Available online 4 December 2021

et al., 2015; Gobiet et al., 2014; Mastrotheodoros et al., 2020) with increasing evidence of higher runoff during fall due to more liquid than solid precipitation and of decreasing summer inflow due to reduced snow-cover, earlier thaw, and glaciers' down wasting (Aili et al., 2019; Beniston and Stoffel, 2014; Confortola et al., 2014). These alterations of the Alpine hydrological regime will substantially negatively impact a wide range of water users, calling for timely adaptation of existing water management strategies (Anghileri et al., 2018; Brekke et al., 2009; Haguma et al., 2014). Climate change adaptation is emerging as a key challenge for the complex infrastructure system controlling water distribution to a variety of multisectoral and often competing water demands, including hydropower production, irrigation supply, flood control, ecological flows, and tourism (Galelli et al., 2010).

In this paper, we analyse the potential vulnerabilities of existing water management strategies in the Po Valley when exposed to changing climate conditions. In particular, the proposed approach is applied to the Lake Como system, one of the most important multi-purpose regulated lakes in Northern Italy.

To quantify the impacts of climate change in the Lake Como system, we implement two different but complementary methods, namely i) a bottom-up approach, i.e. a set of scenarios generated by independently re-sampling the main climatic variables over predefined ranges of variability, ii) a top-down approach, i.e. a simulation-based analysis relying upon an ensemble of IPCC scenarios simulated by global circulation models (GCMs) and properly downscaled to represent the local conditions of the study area.

Through the first method, we evaluate the robustness of the system against a wide range of potential changes in a single or in few climatic drivers. However, such method explores first order (i.e. changes of the mean values) variability and does not consider i) mutual interactions between climate variables such as temperature and precipitation nor ii) higher-order (e.g. changes in variance) effects, changing seasonal patterns or frequency of extreme events (storms, wet/dry spells, heat waves). Thus, they do not represent physically consistent patterns of climate and do not explore full potential variability thereby (Brown and Wilby, 2012; Culley et al., 2016; Prudhomme et al., 2010). The second method instead considers physically based, plausible scenarios, including interconnection between weather variables, and higher-order variability (changes in the variance, seasonal behaviour, frequency distribution, etc.). They are however less useful to identify sensitivity to single drivers, and they need local downscaling, especially for precipitation (Groppelli et al., 2011a).

To pursue our top-down approach, we consider here IPCC climate change scenarios relative to the Fifth Assessment Report (AR5),

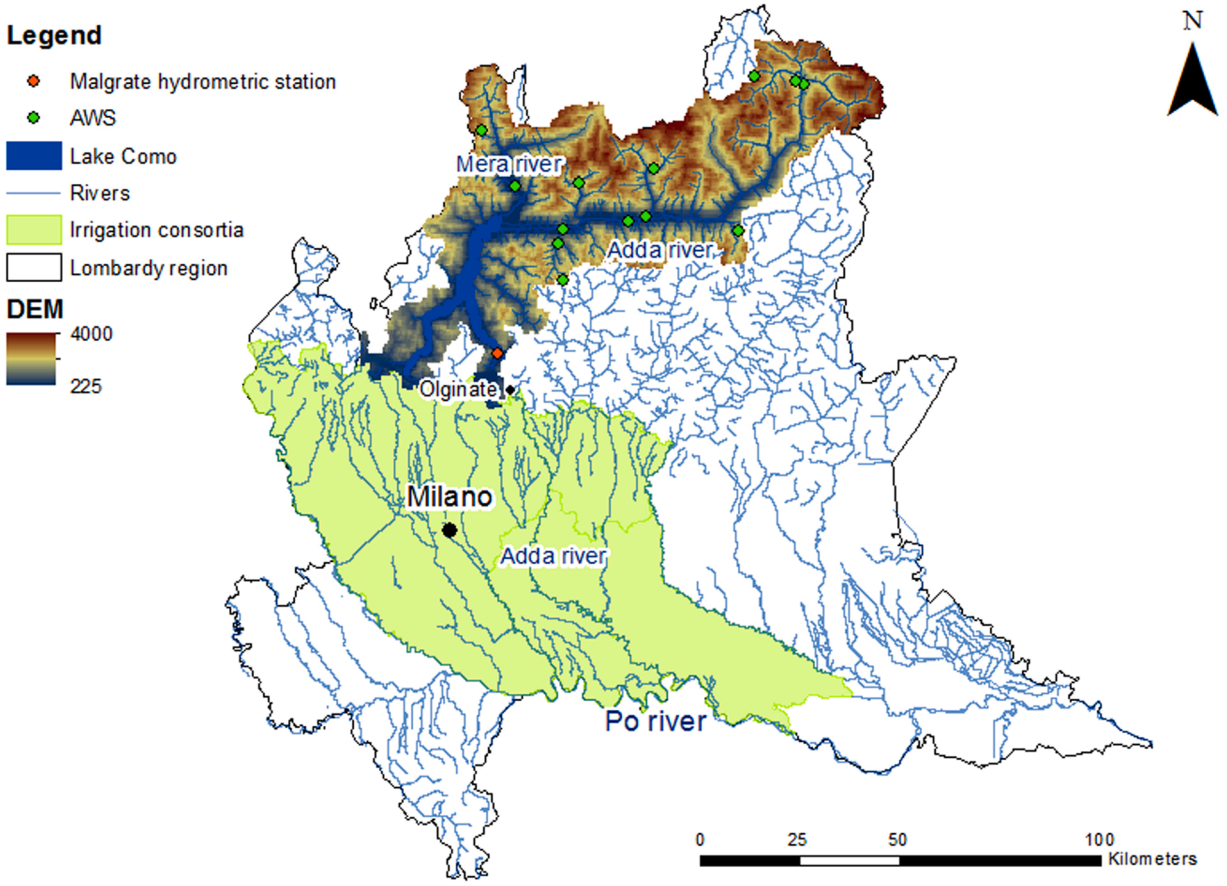


**Fig. 1.** Digital Elevation Model and location of Lake Como catchment. Green points correspond to automatic weather stations, whereas the orange point is the Malgrate hydrometric station. The main irrigation consortia of the Po valley are reported in green. (For interpretation of the references to colour in this figure legend, the reader is referred to the web version of this article.)

and the Sixth Assessment Report (AR6). AR6 couples shared socio-economic pathways (SSPs), that consider e.g. investments in education, health and energy development, with updated representative concentration pathways (RCPs, already used in the AR5), relative to greenhouse gases (GHG) emissions, and land use changes scenarios (Fuso et al., 2021). The use of different AR5/AR6 IPCC scenarios (RCPs/SSPs) as input to different climate and hydrological models, may broaden the projection range, and uncertainty thereby (Herman et al., 2020). Finally, to evaluate the main sources of variability of our projected scenarios we carry out an uncertainty analysis using the ANOVA method.

Since the choice of a specific hydrological model may bias the analysis of the projected hydrologic regimes, in our analysis we use two hydrological models, namely *Topkapi* (Fatichi et al., 2015) and *Poli-Hydro* (Aili et al., 2019; Soncini et al., 2017).

The rest of the paper is organized as follows. In the next section, we introduce the case study area and the data used. Then, the methodology is explained in Section 3. The results are discussed in Section 4, and in Section 5 main findings and conclusions are given.

## 2. Case study

The case study area is the Lake Como system (Fig. 1), located between the Central Italian Alps, and the agricultural districts of the Po valley. The lake has an estimated volume of ca. 23.4 $km^3$ and it is operated at the Olginate dam under multiple constraints (Anghileri et al., 2011; Denaro et al., 2017; Giuliani et al., 2016b; Giuliani and Castelletti, 2016). The lake release supplies downstream water demand to hydroelectric plants and to four irrigation districts over an area of 1400 $km^2$, with maxima in June and July (ca. 226 $m^3s^{-1}$), and minima in winter nearby 90 $m^3s^{-1}$. These values correspond to the water rights negotiated by the different negotiation consortia. Main cultivated crops are maize, grassland, rice, wheat, sugar beets, with production comparable to the most productive areas of Europe (East Flanders, Alsace, Noord-Bradant, and Schleswig-Holstein, Bocchiola et al. 2013; Bocchiola, 2015).

The second objective of the lake management is to avoid shoreline floods, i.e. by maintaining lake level below the lowest point on the lake shores in the city of Como, corresponding to a water stage of 1.24 m (referred to hydrometric zero, 197.37 m asl, (Giuliani et al., 2016b). Management of the lake is constrained with a downstream ecological flow of 5 $m^3s^{-1}$ (Denaro et al., 2017). Operation therein aims at minimizing the irrigation deficit with respect to demand, and the yearly number of days with shoreline floods, considering a small regulation capacity (average inflow-to-capacity ratio of 6%, Anghileri et al. 2011).

Lake Como collects water from the large Adda river catchment draining an area of 4438 $km^2$, between Italy and Switzerland (90%, and 10%, respectively), and with an altitude range between 255 m asl, and 4000 m asl. The lake is laid within a temperate region, but the catchment has a cold climate in the mountain areas, and largely cryosphere-driven hydrology (Aili et al., 2019; Bombelli et al., 2019; Peel et al., 2007).

### 2.1. Data

Meteorological data are used as input to the hydrological models (*Poli-Hydro PH*, and *Topkapi-ETH TPK*). The driving variables are

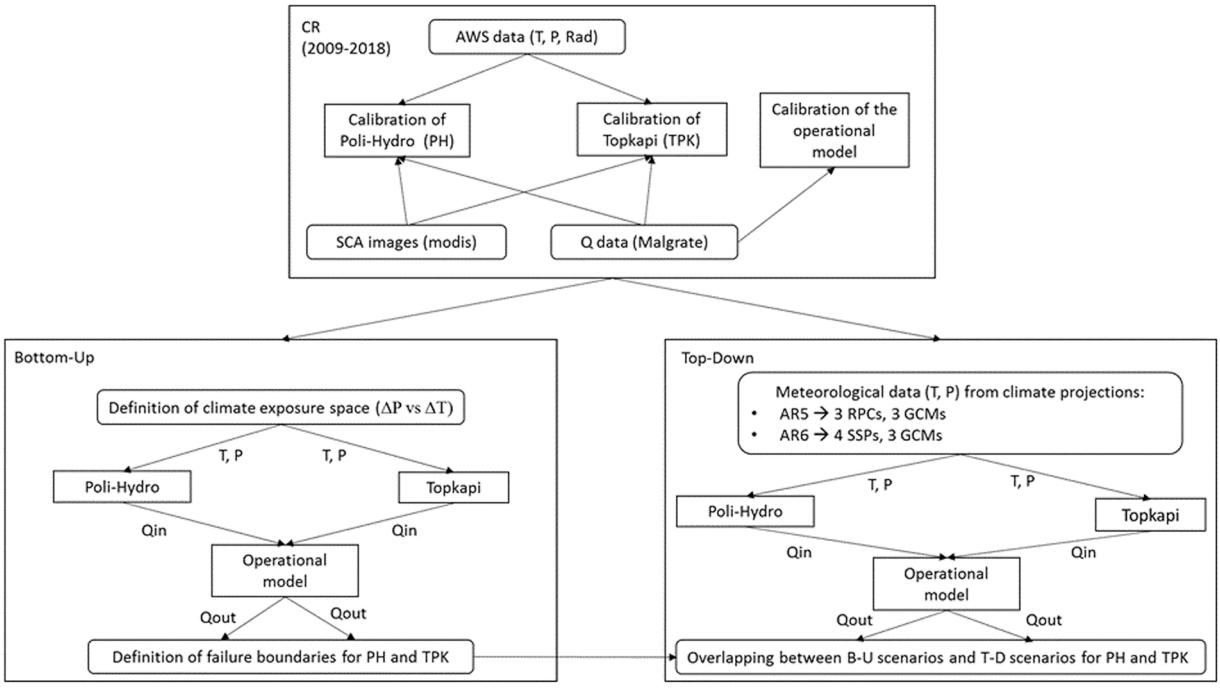


**Fig. 2.** Flowchart of the methodology. Acronyms explained in the text.

temperature (*T*), precipitation (*P*) and geographic (topographically corrected) radiation (*Rad*). These data were collected for a control run (CR) period (2009–2018), as made available from the automatic weather stations (AWS) grid of ARPA Lombardia (the regional protection agency for the environment). Daily data are available from 13 AWSs, homogeneously distributed in the case study area. For model tuning, daily inlet discharges to Lake Como are used. Such data were provided by the Consorzio dell'Adda (a consortium managing the lake outlet) and obtained using inverse flow routing, starting from collected data at the hydrometer in Malgrate. Moreover, satellite images of snow-covered area (*SCA*) were collected for the entire CR period, every two weeks from March 14th to June 18th. These images were acquired by the sensor MODIS (Moderate Resolution Imaging Spectroradiometer) on board the satellite Terra.

## 3. Methodology

We focus upon the impact of hydrological changes, driven by prospective climate change, upon lake operation. Such impact was quantified using indexes of operation failure. For this purpose, we set-up two hydrological models (*Poli-Hydro* and *Topkapi-ETH*) to simulate the inlet discharge to the lake (necessary for benchmarking against future hydrological scenarios, also obtained using these hydrological models). An operational model of the lake is tuned against the historical operational data to closely mimicking historical operation patterns.

Subsequently, we benchmark operation efficiency against prospective climate, and hydrology, under the proposed two-fold approach, namely by i) bottom-up B-U, obtained by making incremental changes to climate variables ($\Delta T$, $\Delta P$), i.e. with a step-wise approach providing a reference exposure space, and ii) top-down T-D, using physically-based climate scenarios, e.g. under the IPCC framework, locally downscaled. We calculate the failures in terms of irrigation deficit and the number of floods under the B-U approach and then benchmark against those under the T-D approach. Climate scenarios are taken from the outputs of global circulation models (GCMs) under the AR5/AR6 of IPCC. We use three GCMs for each AR, three representative concentration pathways (RCPs) for AR5, and four shared socioeconomic pathways (SSPs) for AR6, for a total of 21 scenarios. For each of these 21 scenarios, two reference periods (with length of thirty years as often required in hydro-climatological analysis) are considered, 2041–2070, half-century P1, and 2071–2100, end of century P2, for a total of 42 projected periods. Each of such climate scenarios is then operated using the two hydrological models, to obtain projected hydrological input to the lake (84 flow series). The methodology is presented in Fig. 2.

### 3.1. Bottom-up and top-down approaches

For each hydrological model, a control run inflow series (i.e. based upon climate during 2009–2018) is generated. From outflow discharge, and lake level, it is possible to verify the fulfilment of ecological flow (always fulfilled in practice in our simulations), irrigation demand (changing with the season, and available daily), and flood protection (i.e. days of flooding), at a daily scale. The incremental step B-U used for temperature is $\Delta T_s = \pm 1\ ^\circ C$, and a range of $\Delta T$ from $-2\ ^\circ C$ to $+8\ ^\circ C$ is considered. For precipitation, a multiplicative correction is applied consistently with the inherently positive nature of rainfall values, in the range of $\Delta P$ from $-15\%$ to $+20\%$ is used, with an incremental step of $\Delta P_s = \pm 5\%$. The range of variation for *T*, *P* is chosen after a preliminary screening based upon the IPCC scenarios, for consistency.

The inlet discharge to Lake Como is simulated for each B-U scenario (i.e. each combination of $\Delta T$, and $\Delta P$), with the two hydrological models previously tuned (pH and *TPK*, see below). Then the same calculation is pursued for the top-down T-D approach, i.e. using climate scenarios as obtained from the GCMs, processed by the hydrological models pH/*TPK*. Here, 3 RCPs of the AR5, and 4 SSPs of the AR6 are used. Series of temperature and precipitation are obtained from 3 GCMs for the AR5, and from the corresponding 3 GCMs for the AR6.

Specifically, we use EC-Earth (Hazeleger et al., 2012), CCSM4 (Gent et al., 2011), and Echam6 (Stevens et al., 2013) from AR5, and EC-Earth3.0 (EC-Earth Consortium (EC-Earth), 2019), CESM2 (Danabasoglu et al., 2020), and Echam6.3 (Mauritsen et al., 2019) for the AR6.

The RCP 2.6, RCP 4.5, and RCP 8.5 are used for the AR5, and SSP 2.6, SSP 4.5, SSP 7.0, and SSP 8.5 are used for the AR6. The daily series of *T*, *P* are downscaled locally (Groppelli et al., 2011a, 2011b), to obtain series of weather variables consistent with the hydrological model spatial resolution. Precipitation is downscaled with a stochastic space random cascade model, which reproduces the mean and the variance of the observed data, whereas temperature is downscaled using a correction with a mean monthly $\Delta T$ approach. Eventually, 21 scenarios are obtained and simulated with each hydrological model, to derive inlet discharges. Then, lake outflow, and level, are simulated via operation. The simulation is carried out for the period 2019–2100, but two representative periods are examined for each scenario, namely 2041–2070, P1, and 2071–2100, P2.

Then, the so obtained 42 T-D scenarios (21 climate scenarios, 2 periods) are overlapped to the 2 exposure spaces (i.e. regular grid for B-U approach, for PH/*TPK*), based upon their average temperature and precipitation variation, with respect to the CR period.

### 3.2. Hydrological models: Poli-Hydro and Topkapi-ETH

Two hydrological models, *Poli-Hydro PH* and *Topkapi TPK*, were previously tuned in this area (Giudici et al., 2020; Fuso et al. 2021, respectively). PH and *TPK* use a regular grid for the simulation of the water budget, and for each cell, they need information on land cover and elevation. Both PH and *TPK* simulate snow, and ice melt using a mixed degree-day approach, based on average daily temperature, and short wave radiation (Aili et al., 2019). While *TPK* considers glacier melt basing on a temperature-index method (Pellicciotti et al., 2005), PH also simulates the dynamics of glaciers, calculating ice flow, and mass balance, and updating glacier

volume and area (Aili et al., 2019; Bombelli et al., 2019). PH uses a single soil layer, with isotropic conductivity (changing with soil saturation), whereas *TPK* considers three layers, and a vertical/horizontal conductivity. Potential evapotranspiration in PH is assessed via Hargreaves' formula, whereas *TPK* uses Priestley-Taylor's equation. To increase the reliability of future projections, it was important to attain a good calibration of the hydrological models and to properly represent the main flow components in the area, especially as given by seasonal snow melt (Krysanova et al., 2020). Accordingly, we pursue model tuning (i.e. for Degree-Day of snow) also based upon observed snow-melt dynamics. We use seasonal snow cover area (*SCA*), as estimated using MODIS images. Multi-targeted model tuning in cryospheric areas results in an accurate description of hydrological processes thereby, so better capturing the impacts of climate changes, especially with respect to temperature, which is the main driver of seasonal cryospheric melting (e.g. Soncini et al. 2017). In Table 1 we report the results of calibration of PH and *TPK* in the control period 2009–2018.

### 3.3. Operational model

The operational model simulates lake operation, i.e. daily releases, and, by solving a mass balance equation with the net inflow to Lake Como, the daily storages, and generates a set of Pareto optimal operations diversely balancing the two targets of flood control and water supply downstream. As a reference policy, we select the one more closely mimicking historical operation patterns, as observed from discharge data at the downstream hydrometer in Malgrate (Li, 2016). This is done to benchmark future operation performance against the presently adopted strategies, rather than against theoretically optimal ones (that are not implemented in practice). The set of optimal operating policies $p*$ at the daily scale is:

$$p* = \underset{p}{\text{argmin}} J = [J^{flo}, J^{irr}], \tag{1}$$

where $p$ is a closed-loop control policy, that for each time step (day) determines water release over the next 24 h, based on the day of the year and lake level, parameterized as a Gaussian radial basis function. The term $p*$ describes alternative regulation of the lake over the historical climate conditions. $J^{flo}$ and $J^{irr}$ are the annual average number of floods [d $y^{-1}$], and the average squared daily water irrigation deficit [$m^3s^{-2}d^{-1}$] (Castelletti et al., 2010, 2008; Denaro et al., 2017; Giuliani et al., 2015, 2016c; Giuliani and Castelletti, 2016). Then, using the operational model, for each year of simulation of the CR period, the number of days with shoreline flooding, and the irrigation deficit are calculated. The value corresponding to the 90th percentile of the deficit/flood distribution (i.e. exceedance in one year out of ten) is used as a reference threshold to benchmark performance (success/failure), under both B-U and T-D approaches (Kasprzyk et al., 2013). The simulation with the operational model is also carried out for each scenario under the B-U approach, to define areas of failure of the system in the exposure space, in terms of irrigation deficit, or flood failure. $J^{flo}$ and $J^{irr}$ are calculated also for the T-D scenarios, to define the differences in failure between the B-U approach and the T-D one.

### 3.4. Analysis of variance

We explore possible sources of uncertainty in projections of climate change impacts upon the hydrology of the Lake Como catchment. Using a large number of climate scenarios and a multi-hydrological-model approach enlarges the potential range of future projections, thereby increasing uncertainty (Krysanova et al., 2020). To quantify the share of variability (uncertainty) brought by each of these components into the hydrological scenarios, we perform a three-way ANOVA (Analysis Of Variance, Aryal et al. 2019). We analyse monthly flows to exploit seasonal differences within flow formation processes and future projections thereby. Total (flow) process variance was expressed as:

$$SST = SS_{hydro} + SS_{GCM} + SS_{RCP,SSP} + SS_{res}. \tag{2}$$

Therein, *SST* is the total sum of squares, $SS_{hydro}$, $SS_{GCM}$, and $SS_{RCP,SSP}$ are the sum of squares referred to the main effects of the hydrological model, GCM and IPCC scenario, respectively. The interaction effects and the sum of squares of residues are quantified into $SS_{res}$, which correspond to the intrinsic variability of the flow variables.

## 4. Results and discussion

### 4.1. Hydrological projections under IPCC climate change scenarios: AR5/AR6

In Figs. 3–5, we report the quantitative link between changes in precipitation, and discharge, distributed seasonally. An increase in total (yearly) precipitation results in an increase in total discharge, and vice versa, a decrease in precipitation leads to a reduction in

**Table 1**
Total bias and NSE for discharge and snow cover area for the period 2009–2018, for both hydrological models, Poli-Hydro and Topkapi.

| | Discharge at inlet section [$m^3s^{-1}$] | | Snow covered area -SCA [%] | |
|---|---|---|---|---|
| | 2009–2018 | | 2009–2018 | |
| | Bias [%] | NSE monthly [-] | Bias [%] | NSE total [-] |
| Poli-Hydro | -3.25% | 0.78 | -6.68 | 0.75 |
| Topkapi | -1.71% | 0.86 | 7.85 | 0.69 |

inflows. However, almost all values are laid below the sector's diagonal, i.e. discharge increases less (or decreases more) than precipitation (Fig. 3). This results from a growth in evapotranspiration, due to higher temperatures (e.g. Groppelli et al. 2011b). Although some scenarios show an increase in annual discharge, summer discharge always decreases (Fig. 4), and more consistently so under AR6 scenarios, than under AR5 scenarios.

Fig. 5 shows that, for a raise in annual discharge, fall discharge increases more than proportionally, and mainly so under AR5 scenarios. Instead, for a decrease in the total discharge, some scenarios still exhibit a positive variation of fall discharge, and others display a little decrease in the latter.

In response to a precipitation increase of + 10–15%, total annual discharge increases (Fig. 3). However, such an increase of + 12–13% does not imply an increase in summer discharge (Fig. 4). Under negative changes in precipitation, lower yearly discharge is foreseen (Fig. 3). However, some scenarios still show fall discharge rising, due to an increase of precipitation in fall (Fig. 5 and Tables 2, 3).

Looking at the results of the ANOVA (Fig. 6, in relative form), under both AR5/AR6, and in both periods P1/P2, uncertainty in flow projection is governed more by climate projections, and internal variability, than by the choice of the hydrological model.

Under AR5 the main source of uncertainty is due to the (choice of the) GCMs, and to the inner (meteo-hydrological) variability, both in P1 and P2 (Fig. 6, a and c). The projected precipitation under AR5 displays somewhat higher variability than under AR6 (Fig. 3). Accordingly, inflows thereby are more largely variable. Under AR6, less variability of precipitation amount is detected with respect to AR5, mainly in P2, so in the rainy season, the uncertainty resulting from the GCM is smaller than those deriving from the internal variability of the meteo-hydrological process, intrinsically variable by nature (Fig. 6d).

Especially at the end of the century in spring and summer, uncertainty is largely governed by the (choice of the) IPCC scenarios (RCPs/SSPs, Fig. 6, c and d). At mid-century, temperature increases similarly for all scenarios, while at the end of the century temperature changes are very different across scenarios, and so the choice of a given scenario is crucial, and choice of GCM becomes less important.

ANOVA results in absolute terms also indicate seasonal uncertainty of inflow projection (Fig. 7). Globally, the total uncertainty increases between P1 and P2, both for AR5 and AR6. October-November, and June-August, show the highest variance/uncertainty, likely due to the influence of the variability of precipitation, and temperature range, respectively.

### 4.2. *Vulnerability analysis*

Figs. 8 and 9 show the exposure space (B-U approach) and the results of the T-D approach using PH and *TPK*. B-U scenarios (circles), and T-D scenarios (AR5 and AR6), for two representative periods (P1, 2041–2070, and P2, 2071–2100) are reported. The B-U scenarios cover the entire exposure space and define the failure regions for number of floods (red region) and irrigation deficit (yellow region). The purple region includes the B-U scenarios, where both objectives display failure, and the blue points represent the region of success (combination of ΔT and ΔP, with no failure). T-D scenarios are overlapped with the same colours, with their proper values of ΔT and ΔP against the CR period.

In the future overall, operation performance declines, in terms of irrigation/flood, for seasonal precipitation decrease/increase. Considering the B-U scenarios, some differences between PH and *TPK* can be seen. PH provides increasing (vs the CR) irrigation deficit for any temperature increase, and precipitation reduction, whereas *TPK* keeps an acceptable performance, for a small decrease of precipitation, and increase of temperature. Focusing upon differences between the B-U scenarios, and T-D scenarios, two main differences can be pointed out. For *Poli-Hydro*, AR5 scenarios with an increase of precipitation between + 10% and + 15% provide (also) increased irrigation deficit, in contrast with the B-U scenarios. For *Topkapi*, likewise the failure in both objectives is observed mainly with a precipitation increase between + 5% and + 10%, both under AR5 and AR6 scenarios. Looking at Figs. 3 and 4, while annual

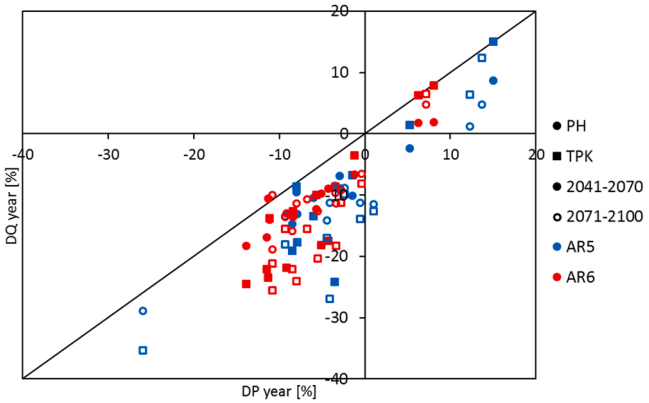


**Fig. 3.** Average discharge variation vs average precipitation variation for each scenario of AR5 (blue) and AR6 (red) at the middle (full) and the end (empty) of the century, for Poli-Hydro (points) and Topkapi (squares) models. (For interpretation of the references to colour in this figure legend, the reader is referred to the web version of this article.)

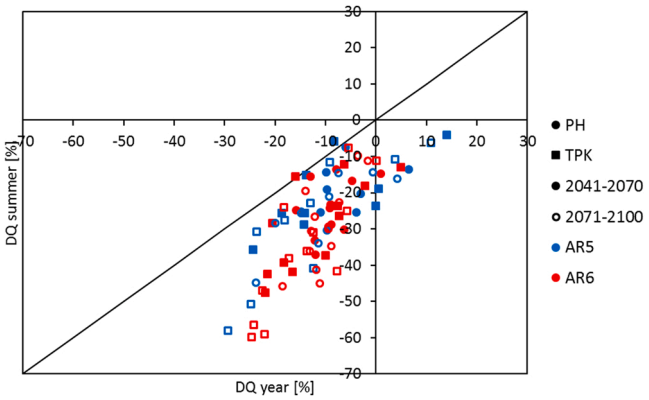


**Fig. 4.** Average summer discharge variation vs average year discharge variation for each scenario of AR5 (blue) and AR6 (red) at the middle (full) and the end (empty) of the century, for Poli-Hydro (points) and Topkapi (squares) models. (For interpretation of the references to colour in this figure legend, the reader is referred to the web version of this article.)

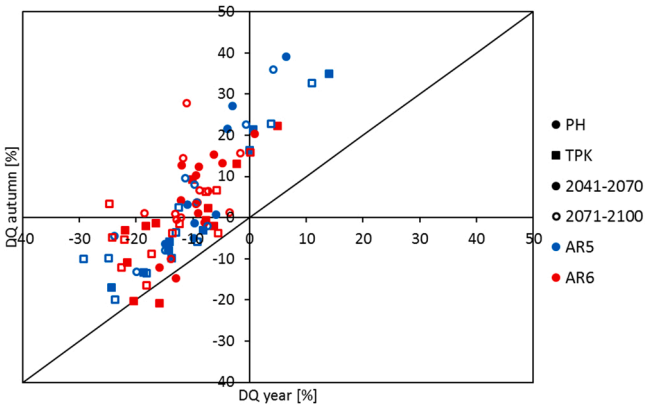


**Fig. 5.** Average autumn discharge variation vs average year discharge variation for each scenario of AR5 (blue) and AR6 (red) at the middle (full) and the end (empty) of the century, for Poli-Hydro (points) and Topkapi (squares) models. (For interpretation of the references to colour in this figure legend, the reader is referred to the web version of this article.)

precipitation, and annual discharge, increase, summer discharge decreases. Thus, (larger) irrigation deficits may still be expected, which were not highlighted in the B-U scenario.

Moreover, for *PH,* flood failures are observed under AR6 scenarios, even with a temperature change of ca. + 6 °C, and a decrease in precipitation down to − 10%, which does not occur under the B-U scenarios. Flood failures under temperature increase higher than + 5 °C (Figs. 8, 9) could derive from an increase in liquid precipitation at the expense of snowfall. Indeed, an increase in fall discharge is seen, in response to increasing liquid precipitation in fall (Fig. 5 and Tables 2, 3). Such results come as a consequence of the seasonal variability of climate (supplementary material, *P* and *T*), as projected by the adopted GCMs under the T-D approach. Such circumstances could bring criticalities in lake operation, undetected when using a B-U approach.

To evaluate the link between climatic variables, seasonal discharges, and operation performance, a correlation analysis is performed (Table 2 for PH, and Table 3 for *TPK*). We consider seasonal climate for CR, P1, and P2, for each GCM and RCP/SSP, and the corresponding inflows, and the final performance indexes (irrigation/flood). In the tables, the significant correlations (significance level of 95%, reported in the supplementary material) that are larger than 0.6, or smaller than − 0.6, are highlighted in bold. Looking at climate variables, as expected seasonal temperatures are highly correlated with yearly temperature, for both PH and *TPK*. Similarly, seasonal precipitation affects seasonal discharge. To assess the degree of correlation between climatic/hydrological variables, and flood failure, we use the daily flooding volume during floods $\Delta H$, more linked to weather and hydrological conditions (rain/stream flows) than the number of days with flood. Our results show that irrigation deficit mainly correlates to summer discharge (−0.62 for PH, −0.84 for *TPK*), and less to summer temperature, and spring/summer precipitation, whereas floods are mostly affected by fall flows, especially for PH (0.62 PH, 0.57 *TPK*).

Figs. 10 and 11 display the magnitude of failure in terms of irrigation deficit, and number of floods for PH and *TPK*, for the 42T-D scenarios here processed (for both PH and *TPK*). The light-blue circles display failure thresholds for the two objectives, calculated as the 90th percentile on the CR period series (2009–2018), as reported above. The threshold values are $Q_t = 801.3$ m$^3$s$^{-1}$ for PH, and $Q_t = 1768.87$ m$^3$s$^{-1}$ for *TPK*, and 52 days for PH and 56 days for *TPK*, for irrigation deficit and flood, respectively.

**Table 2**
Correlation analysis for the simulation with Poli-Hydro model. In bold significant values $> 0.6$ and $< -0.6$.

| | Qw | Qsp | Qsu | Qa | Qy | Tw | Tsp | Tsu | Ta | Ty | Pw | Psp | Psu | Pa | Py | ID | ΔH |
|---|---|---|---|---|---|---|---|---|---|---|---|---|---|---|---|---|---|
| **Qwinter** | 1.00 | 0.16 | -0.08 | 0.02 | 0.31 | 0.35 | 0.22 | 0.28 | 0.23 | 0.34 | 0.42 | -0.02 | -0.05 | 0.04 | 0.24 | -0.03 | 0.03 |
| **Qspring** | | 1.00 | 0.26 | 0.00 | 0.52 | -0.26 | -0.30 | -0.28 | -0.10 | -0.30 | 0.19 | **0.75** | 0.12 | -0.01 | 0.50 | -0.59 | 0.07 |
| **Qsummer** | | | 1.00 | 0.07 | 0.52 | -0.24 | -0.34 | -0.45 | -0.16 | -0.39 | 0.03 | 0.26 | **0.77** | -0.02 | 0.53 | **-0.62** | 0.09 |
| **Qautumn** | | | | 1.00 | **0.68** | 0.10 | 0.13 | 0.09 | 0.15 | 0.13 | -0.05 | 0.04 | 0.17 | **0.94** | **0.62** | -0.06 | **0.62** |
| **Qyear** | | | | | 1.00 | -0.06 | -0.14 | -0.19 | 0.05 | -0.12 | 0.18 | 0.48 | 0.55 | 0.59 | **0.95** | **-0.61** | 0.47 |
| **Twinter** | | | | | | 1.00 | 0.57 | **0.61** | 0.35 | **0.79** | 0.04 | -0.06 | -0.10 | 0.08 | -0.01 | 0.34 | 0.07 |
| **Tspring** | | | | | | | 1.00 | **0.75** | 0.43 | **0.86** | 0.02 | -0.27 | -0.15 | 0.12 | -0.11 | 0.47 | 0.06 |
| **Tsummer** | | | | | | | | 1.00 | 0.45 | **0.91** | 0.00 | -0.22 | -0.34 | 0.11 | -0.20 | 0.55 | 0.06 |
| **Tautumn** | | | | | | | | | 1.00 | 0.57 | 0.06 | -0.04 | -0.04 | 0.11 | 0.05 | 0.12 | 0.06 |
| **Tyear** | | | | | | | | | | 1.00 | 0.02 | -0.19 | -0.22 | 0.13 | -0.11 | 0.49 | 0.08 |
| **Pwinter** | | | | | | | | | | | 1.00 | 0.03 | 0.03 | -0.04 | 0.19 | -0.11 | -0.03 |
| **Pspring** | | | | | | | | | | | | 1.00 | 0.16 | 0.03 | 0.56 | **-0.62** | 0.07 |
| **Psummer** | | | | | | | | | | | | | 1.00 | 0.01 | **0.62** | **-0.60** | 0.09 |
| **Pautumn** | | | | | | | | | | | | | | 1.00 | 0.56 | 0.01 | 0.55 |
| **Pyear** | | | | | | | | | | | | | | | 1.00 | **-0.65** | 0.38 |
| **Irrigation deficit** | | | | | | | | | | | | | | | | 1.00 | -0.01 |
| **ΔH flood** | | | | | | | | | | | | | | | | | 1.00 |

**Table 3**
Correlation analysis for the simulation with Topkapi model. In bold significant values $> 0.6$ and $< -0.6$.

| | Qw | Qsp | Qsu | Qa | Qy | Tw | Tsp | Tsu | Ta | Ty | Pw | Psp | Psu | Pa | Py | ID | ΔH |
|---|---|---|---|---|---|---|---|---|---|---|---|---|---|---|---|---|---|
| **Qwinter** | 1.00 | 0.28 | 0.04 | 0.11 | 0.39 | 0.36 | 0.23 | 0.26 | 0.21 | 0.33 | 0.39 | 0.01 | -0.04 | 0.06 | 0.25 | -0.06 | 0.14 |
| **Qspring** | | 1.00 | 0.52 | 0.18 | **0.73** | -0.20 | -0.30 | -0.30 | -0.01 | -0.28 | 0.23 | **0.82** | 0.22 | 0.02 | **0.61** | **-0.71** | 0.19 |
| **Qsummer** | | | 1.00 | 0.28 | **0.75** | -0.26 | -0.39 | -0.51 | -0.15 | -0.43 | 0.09 | 0.43 | **0.87** | 0.00 | **0.69** | **-0.84** | 0.19 |
| **Qautumn** | | | | 1.00 | **0.69** | 0.05 | 0.06 | -0.01 | 0.14 | 0.06 | 0.00 | 0.13 | 0.33 | **0.89** | **0.73** | -0.25 | 0.57 |
| **Qyear** | | | | | 1.00 | -0.07 | -0.19 | -0.27 | 0.05 | -0.18 | 0.21 | 0.54 | 0.59 | 0.45 | **0.92** | **-0.74** | 0.45 |
| **Twinter** | | | | | | 1.00 | 0.57 | **0.61** | 0.35 | **0.79** | 0.04 | -0.06 | -0.10 | 0.08 | -0.01 | 0.34 | 0.04 |
| **Tspring** | | | | | | | 1.00 | **0.75** | 0.43 | **0.86** | 0.02 | -0.27 | -0.15 | 0.12 | -0.11 | 0.48 | 0.04 |
| **Tsummer** | | | | | | | | 1.00 | 0.45 | **0.91** | 0.00 | -0.22 | -0.34 | 0.11 | -0.20 | 0.58 | 0.01 |
| **Tautumn** | | | | | | | | | 1.00 | 0.57 | 0.06 | -0.04 | -0.04 | 0.11 | 0.05 | 0.11 | 0.09 |
| **Tyear** | | | | | | | | | | 1.00 | 0.02 | -0.19 | -0.22 | 0.13 | -0.11 | 0.51 | 0.05 |
| **Pwinter** | | | | | | | | | | | 1.00 | 0.03 | 0.03 | -0.04 | 0.19 | -0.11 | 0.02 |
| **Pspring** | | | | | | | | | | | | 1.00 | 0.16 | 0.03 | 0.56 | **-0.60** | 0.14 |
| **Psummer** | | | | | | | | | | | | | 1.00 | 0.01 | 0.62 | **-0.65** | 0.16 |
| **Pautumn** | | | | | | | | | | | | | | 1.00 | **0.56** | -0.01 | 0.48 |
| **Pyear** | | | | | | | | | | | | | | | 1.00 | **-0.67** | 0.44 |
| **Irrigation deficit** | | | | | | | | | | | | | | | | 1.00 | -0.12 |
| **ΔH flood** | | | | | | | | | | | | | | | | | 1.00 |

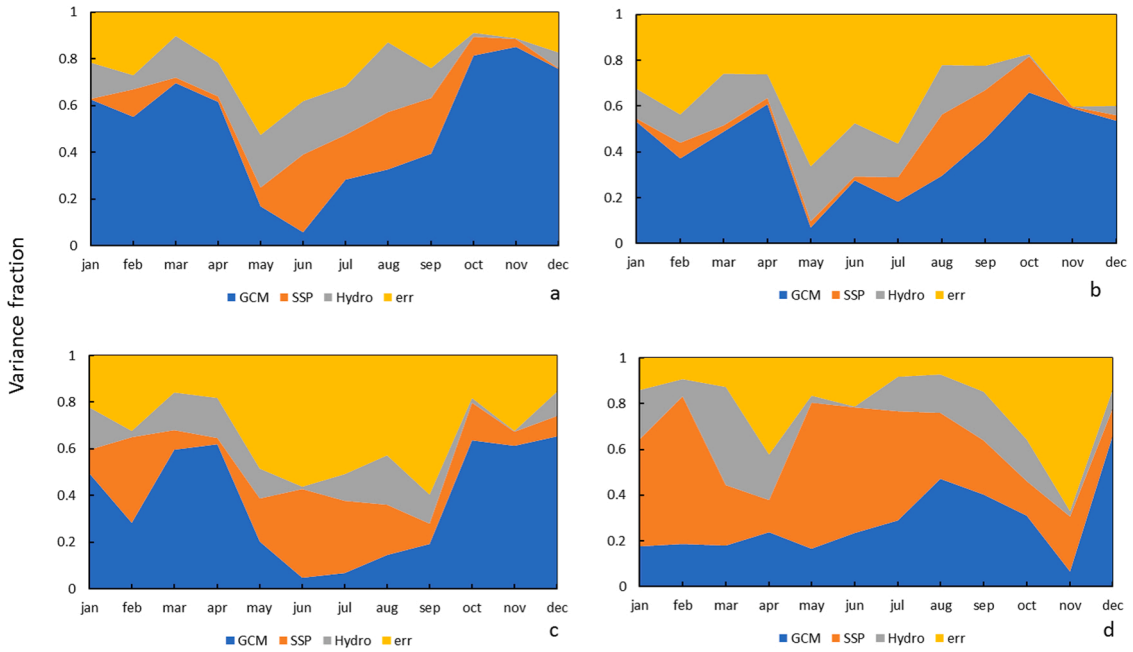


**Fig. 6.** Variance fraction of different sources of uncertainty. (a) AR5, mid-century. (b) AR6, mid-century. (c) AR5, end-of-century. (d) AR6, end-of-century.

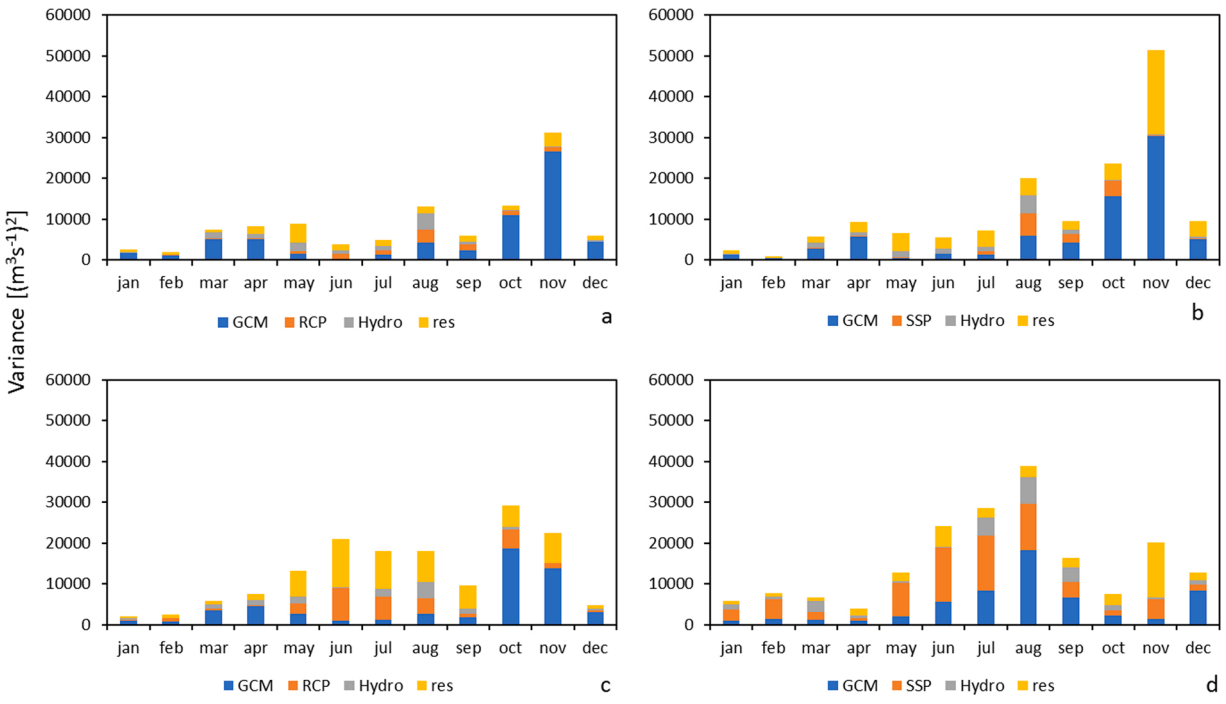


**Fig. 7.** Absolute uncertainty for 3 GCMs. (a) AR5, mid-century. (b) AR6, mid-century. (c) AR5, end-of-century. (d) AR6, end-of-century.

Results show that the most critical condition in terms of irrigation deficit is given under AR6 scenarios (with $\Delta T$ of approx. $+6$ °C), with the highest values for *TPK* than for PH. Concerning flood failure, PH, and *TPK* provide similar outcomes with respect to the AR5 scenarios. The main differences occur between AR5 and AR6, since *TPK* exhibits flood failure mainly under AR5 scenarios. The threshold values for the two objectives are calculated also considering the observed inflow data during CR 2009–2018, resulting in $Q_t = 1212.25\ m^3s^{-1}$ for irrigation deficit, and 51 days of shoreline flood.

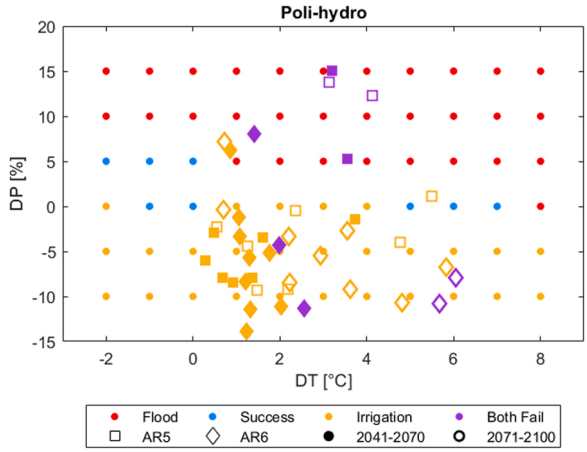


**Fig. 8.** Failure regions considering synthetic scenarios and the failure for climate change scenarios. Here, the simulation is done with Poli-Hydro model. Red represents the flood failure, yellow the irrigation demand failure, blue no failure and purple both failures. Squares represent AR5 scenarios, whereas diamonds provide AR6 scenarios. Full squares/diamonds represent the 2041–2070 period, and empty squares/diamonds represent the 2071–2100 period. (For interpretation of the references to colour in this figure legend, the reader is referred to the web version of this article.)

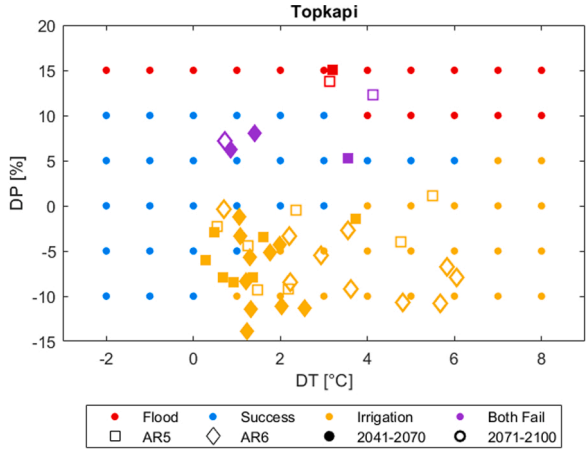


**Fig. 9.** Failure regions considering synthetic scenarios and the failure for climate change scenarios. Here, the simulation is done with the TPK model. Red represents the flood failure, yellow the irrigation demand failure, blue no failure and purple both failures. Squares represent AR5 scenarios, whereas diamonds provide AR6 scenarios. Full squares/diamonds represent the 2041–2070 period, and empty squares/diamonds represent the 2071–2100 period. (For interpretation of the references to colour in this figure legend, the reader is referred to the web version of this article.)

Thresholds for flood failure days is almost the same for PH/*TPK*. Instead, the irrigation failure threshold $Q_t$ is quite different for PH and *TPK*, and the value from observations is an average between the two, which depends clearly upon the different flow dynamics as depicted by the two models (inflow values, and flow volumes in time, affecting reservoir's management). However, under future climate projections, we detected large failures, not comparable with the historical ones. Accordingly, the disturbance given by using hydrologically modelled flows is lower than the changes resulting from climatic scenarios, e.g. the loss of effectiveness of the current operation policies in the future is higher than the perturbation caused by the (choice of the) hydrological model.

## 5. Conclusions

The bottom-up approach pursued here, relatively easy to implement, is largely used in climate change impact assessment exercise (Brown et al., 2012; Culley et al., 2016; Prudhomme et al., 2010), namely to provide the sensitivity of a system to the changing climate, and possibly to propose a simplified range of future projections to decision-makers. The use of physically-based scenarios (T-D approach) implies larger work, to collect GCMs projections, and subsequently downscale them. A large number of T-D scenarios is necessary and, as a consequence, one also needs to carry out time-consuming hydrological simulations for each scenario (however, several simulations are necessary also for the B-U approach). Moreover, the choice of the GCMs ensembles may influence the results of

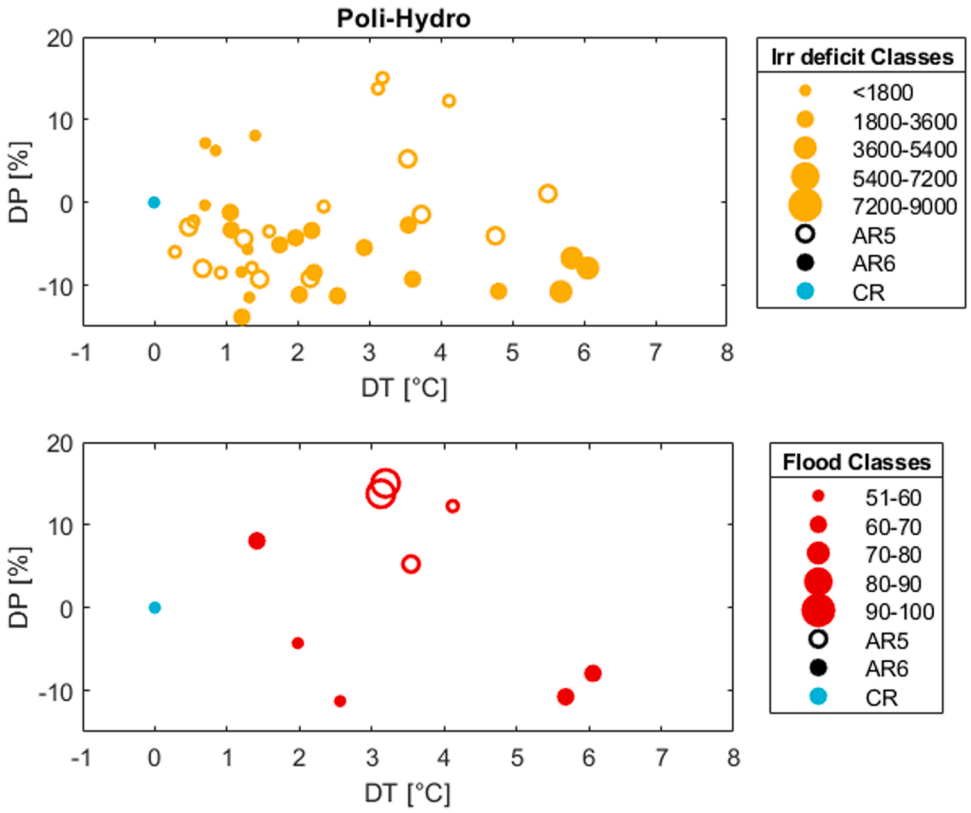


**Fig. 10.** Value of the failure in terms of irrigation deficit and number of floods, for Poli-Hydro, for 42 scenarios (each GCM, each scenario, for AR5 and AR6, at the middle and at the end of the century). Empty points for AR5 and full points for AR6. In light blue is reported the value of the failure for the CR period. (For interpretation of the references to colour in this figure legend, the reader is referred to the web version of this article.)

the assessment (Brown et al., 2012).

In this work, we demonstrate that the results of a T-D approach highlights some criticalities of the system that the B-U approach does not display. This is due to the non-linear influence of climate change as projected, upon seasonality and amount of precipitation, snow accumulation and melt thereby (also mediated by temperature), and modified frequency/extent of flood/drought events.

For instance, changing in timing, and seasonality of precipitation is an important aspect to consider in hydrological projections (for its effect on discharge), that homogeneous (linear) changes in the average values cannot identify (Christensen and Lettenmaier, 2007; Ecmwf, 2019; Quinn et al., 2018). In the supplementary material to this paper, seasonal variation of temperature, and precipitation and the effect upon inflow at Lake Como is reported. The use of a T-D scenario allows to explore physically based, complex scenarios of climate variability, and the impact upon hydrological systems (Manning et al., 2009), and therefore the gain of information obtained by considering IPCC (or anyway, physically based) scenarios for proper climate change impact assessment, and decision making can be highlighted. The results of our ANOVA test are coherent with other studies (see e.g. Wiley and Palmer, 2008; Anghileri et al. 2011; Aryal et al. 2019), in that they identify in the (choice of) any given GCM, the largest source of uncertainty in the short term. Fig. 6 here however shows that the influence of GCM choice is less relevant under AR6 than under AR5. This may indicate that the (increased) consistency of global circulation modelling under AR6 may result in less spreading of climate/hydrological projections under the same SSP. This is a desirable feature when it comes to the reduction of uncertainty in the assessment of hydrological projections, and subsequent operation performance.

To further improve this work, one may consider using more climate models (including e.g. regional models), and more hydrological models. Albeit using only two models does not provide a full multi-model analysis, it may increase our confidence in the projected hydrological conditions, and highlight the contribution of the model's choice to the uncertainty of projections (Krysanova et al., 2020). Also, in pursuing the T-D approach, different downscaling approaches may be explored, especially critical for precipitation. The downscaling method adopted here is statistical (see. Groppelli et al. 2011b, 2011a) but other methods may be considered. On the other side, the B-U approach may be revised as well, to include non-linearity of the system.

Also, a refined evaluation of the future potential irrigation demand may be done. In the future, under climate change scenarios, an increase of evapotranspiration, as driven by the increase of temperature, and a reduction of summer precipitation in the irrigated area of Po Valley is expected, with a consequent potential increase of water demand for crop irrigation (Bocchiola, 2015). For this reason, the irrigation deficit from Lake Como could be higher. Eventually, one potential solution could be a change of crop from a high water demanding to a less water demanding species. On the other hand, re-optimization of the Lake Como dam operation could help to

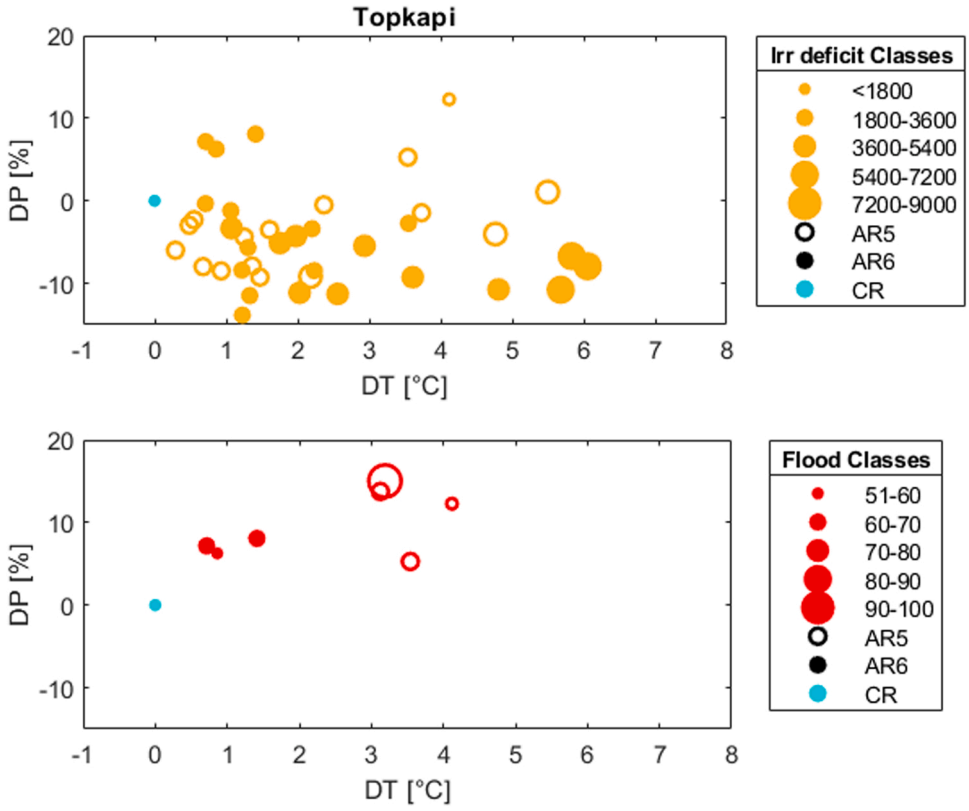


**Fig. 11.** Value of the failure in terms of irrigation deficit and number of floods, for Topkapi, for 42 scenarios (each GCM, each scenario, for AR5 and AR6, at the middle and at the end of the century). Empty points for AR5 and full points for AR6. In light is reported the value of the failure for the CR period.

reduce this problem (Culley et al., 2016), and further effort may be devoted thereby.

Our results here, albeit preliminary and amenable to improvement, notwithstanding provide a possibly dependable tool to assess vulnerable lake operation under climate change during the XXI century, especially when adopting a T-D approach as we did here, and to support the implementation of adaptation strategies from policy makers. Also, the template we propose may be applied to other lakes/reservoirs within the Alps, and other areas, to preliminarily assess water management under climate change henceforth.

## Funding

This work received no external funding.

## CRediT authorship contribution statement

**F.C.**: Conceptualization, Methodology, Software, Formal analysis, Investigation, Resources, Data curation, Visualization, Writing – original draft; **F.F.**: Conceptualization, Methodology, Software, Formal analysis, Investigation, Resources, Data curation, Visualization, Writing – original draft; **M.G.**: Conceptualization, Methodology, Software, Validation, Writing – review & editing, Supervision; **A. C.**: Conceptualization, Methodology, Validation, Writing – review & editing, Supervision; **D.B.**: Conceptualization, Methodology, Validation, Writing – review & editing, Supervision.

## Code availability

Available under request.

## Ethical approval

This chapter does not contain any studies with human participants or animals performed by any of the authors.

## Consent to participate

Not applicable.

## Consent to publish

Not applicable.

## Declaration of Competing Interest

The authors declare no competing interests.

## Data Availability

Available under request.

## Acknowledgments

F.F. acknowledges support from Gruppo CAP Holding Milano through the PhD scholarship "Assessment of hydrological flows in Lombardy Alpine rivers, and their connection with the underground aquifer, under potential climate change scenarios in the XXI century". Climate-Lab, the interdisciplinary laboratory on climate change of Politecnico di Milano (www.climatelab.polimi.it/), is kindly acknowledged for the support. C.F. acknowledges support from the GE.RI.KO. Mera Interreg Project. The authors acknowledge ETH for the use of the *Topkapi-ETH* model.

## Appendix A. Supporting information

Supplementary data associated with this article can be found in the online version at doi:10.1016/j.ejrh.2021.100973.

## References

Aili, T., Soncini, A., Bianchi, A., Diolaiuti, G., D'Agata, C., Bocchiola, D., 2019. Assessing water resources under climate change in high-altitude catchments: a methodology and an application in the Italian Alps. Theor. Appl. Climatol. 135, 135–156. https://doi.org/10.1007/s00704-017-2366-4.

Anghileri, D., Botter, M., Castelletti, A., Weigt, H., Burlando, P., 2018. A comparative assessment of the impact of climate change and energy policies on alpine hydropower. Water Resour. Res. 54, 9144–9161. https://doi.org/10.1029/2017WR022289.

Anghileri, D., Pianosi, F., Soncini-Sessa, R., 2011. A framework for the quantitative assessment of climate change impacts on water-related activities at the basin scale. Hydrol. Earth Syst. Sci. 15, 2025–2038. https://doi.org/10.5194/hess-15-2025-2011.

Aryal, A., Shrestha, S., Babel, M.S., 2019. Quantifying the sources of uncertainty in an ensemble of hydrological climate-impact projections. Theor. Appl. Climatol. 135, 193–209. https://doi.org/10.1007/s00704-017-2359-3.

Beniston, M., Stoffel, M., 2014. Assessing the impacts of climatic change on mountain water resources. Sci. Total Environ. 493, 1129–1137. https://doi.org/10.1016/j.scitotenv.2013.11.122.

Bocchiola, D., 2015. Impact of potential climate change on crop yield and water footprint of rice in the Po valley of Italy. Agric. Syst. 139, 223–237. https://doi.org/10.1016/j.agsy.2015.07.009.

Bocchiola, D., 2014. Long term (1921-2011) hydrological regime of Alpine catchments in Northern Italy. Adv. Water Resour. 70, 51–64. https://doi.org/10.1016/j.advwatres.2014.04.017.

Bocchiola, D., Nana, E., Soncini, A., 2013. Impact of climate change scenarios on crop yield and water footprint of maize in the Po valley of Italy. Agric. Water Manag. 116, 50–61. https://doi.org/10.1016/j.agwat.2012.10.009.

Bombelli, G.M., Soncini, A., Bianchi, A., Bocchiola, D., 2019. Potentially modified hydropower production under climate change in the Italian Alps. Hydrol. Process. 33, 2355–2372. https://doi.org/10.1002/hyp.13473.

Brekke, L.D., Maurer, E.P., Anderson, J.D., Dettinger, M.D., Townsley, E.S., Harrison, A., Pruitt, T., 2009. Assessing reservoir operations risk under climate change. Water Resour. Res. 45. https://doi.org/10.1029/2008WR006941.

Brown, C., Ghile, Y., Laverty, M., Li, K., 2012. Decision scaling: linking bottom-up vulnerability analysis with climate projections in the water sector. Water Resour. Res. 48, 2011WR011212 https://doi.org/10.1029/2011WR011212.

Brown, C., Wilby, R.L., 2012. An alternate approach to assessing climate risks. Eos Trans. Am. Geophys. Union 93, 401–402. https://doi.org/10.1029/2012EO410001.

Castelletti, A., Galelli, S., Restelli, M., Soncini-Sessa, R., 2010. Tree-based reinforcement learning for optimal water reservoir operation. Water Resour. Res. 46. https://doi.org/10.1029/2009WR008898.

Castelletti, A., Pianosi, F., Soncini-Sessa, R., 2008. Water reservoir control under economic, social and environmental constraints. Automatica 44, 1595–1607. https://doi.org/10.1016/j.automatica.2008.03.003.

Christensen, N.S., Lettenmaier, D.P., 2007. A multimodel ensemble approach to assessment of climate change impacts on the hydrology and water resources of the Colorado River Basin. Hydrol. Earth Syst. Sci. 11, 1417–1434. https://doi.org/10.5194/hess-11-1417-2007.

Confortola, G., Soncini, A., Bocchiola, D., 2014. Climate change will affect hydrological regimes in the Alps. Rev. Géogr. Alp 101. https://doi.org/10.4000/rga.2176.

Culley, S., Noble, S., Yates, A., Timbs, M., Westra, S., Maier, H.R., Giuliani, M., Castelletti, A., 2016. Maximum operational adaptive capacity. Water Resour. Res. 52, 6751–6768. https://doi.org/10.1002/2015WR018253.Received.

Danabasoglu, G., Lamarque, J.F., Bacmeister, J., Bailey, D.A., DuVivier, A.K., Edwards, J., Emmons, L.K., Fasullo, J., Garcia, R., Gettelman, A., Hannay, C., Holland, M.M., Large, W.G., Lauritzen, P.H., Lawrence, D.M., Lenaerts, J.T.M., Lindsay, K., Lipscomb, W.H., Mills, M.J., Neale, R., Oleson, K.W., Otto-Bliesner, B., Phillips, A.S., Sacks, W., Tilmes, S., van Kampenhout, L., Vertenstein, M., Bertini, A., Dennis, J., Deser, C., Fischer, C., Fox-Kemper, B., Kay, J.E., Kinnison, D.,

Kushner, P.J., Larson, V.E., Long, M.C., Mickelson, S., Moore, J.K., Nienhouse, E., Polvani, L., Rasch, P.J., Strand, W.G., 2020. The community earth system model version 2 (CESM2). J. Adv. Model. Earth Syst. 12 https://doi.org/10.1029/2019MS001916.
Denaro, S., Anghileri, D., Giuliani, M., Castelletti, A., 2017. Informing the operations of water reservoirs over multiple temporal scales by direct use of hydro-meteorological data. Adv. Water Resour. 103, 51–63. https://doi.org/10.1016/j.advwatres.2017.02.012.
EC-Earth Consortium (EC-Earth), 2019. EC-Earth-Consortium EC-Earth3-Veg model output prepared for CMIP6 ScenarioMIP'. Version 22/10/2020. Earth Syst. Grid Fed. https://doi.org/10.22033/ESGF/CMIP6.727.
Ecmwf, 2019. European State of the Climate 2019 – summary.
Fatichi, S., Rimkus, S., Burlando, P., Bordoy, R., Molnar, P., 2015. High-resolution distributed analysis of climate and anthropogenic changes on the hydrology of an Alpine catchment. J. Hydrol. 525, 362–382. https://doi.org/10.1016/J.JHYDROL.2015.03.036.
Fuso, F., Casale, F., Giudici, F., Bocchiola, D., 2021. Future hydrology of the cryospheric driven Lake Como Catchment in Italy under climate change scenarios. Climate 9, 8. https://doi.org/10.3390/cli9010008.
Galelli, S., Gandolfi, C., Soncini-Sessa, R., Agostani, D., 2010. Building a metamodel of an irrigation district distributed-parameter model. Agric. Water Manag. 97, 187–200. https://doi.org/10.1016/J.AGWAT.2009.09.007.
Gaudard, L., Romerio, F., Dalla Valle, F., Gorret, R., Maran, S., Ravazzani, G., Stoffel, M., Volonterio, M., 2014. Climate change impacts on hydropower in the Swiss and Italian Alps. Sci. Total Environ. 493, 1211–1221. https://doi.org/10.1016/j.scitotenv.2013.10.012.
Gent, P.R., Danabasoglu, G., Donner, L.J., Holland, M.M., Hunke, E.C., Jayne, S.R., Lawrence, D.M., Neale, R.B., Rasch, P.J., Vertenstein, M., Worley, P.H., Yang, Z.L., Zhang, M., 2011. The community climate system model version 4. J. Clim. 24, 4973–4991. https://doi.org/10.1175/2011JCLI4083.1.
Giuliani, M., Castelletti, A., 2016. Is robustness really robust? How different definitions of robustness impact decision-making under climate change. Clim. Change 135, 409–424. https://doi.org/10.1007/s10584-015-1586-9.
Giuliani, Matteo, Castelletti, A., Pianosi, F., Mason, E., Reed, P.M., 2016c. Curses, tradeoffs, and scalable management: advancing evolutionary multiobjective direct policy search to improve water reservoir operations. J. Water Resour. Plan. Manag. 142, 04015050. https://doi.org/10.1061/(ASCE)WR.1943-5452.0000570.
Giuliani, M., Li, Y., Castelletti, A., Gandolfi, C., 2016a. A coupled human-natural systems analysis of irrigated agriculture under changing climate. Water Resour. Res. 52, 6928–6947. https://doi.org/10.1002/2016WR019363.
Giuliani, M., Li, Y., Cominola, A., Denaro, S., Mason, E., Castelletti, A., 2016b. A matlab toolbox for designing multi-objective optimal operations of water reservoir systems. Environ. Model. Softw. 85, 293–298. https://doi.org/10.1016/j.envsoft.2016.08.015.
Giuliani, M., Pianosi, F., Castelletti, A., 2015. Making the most of data: an information selection and assessment framework to improve water systems operations. Water Resour. Res. 51, 9073–9093. https://doi.org/10.1002/2015WR017044.
Gobiet, A., Kotlarski, S., Beniston, M., Heinrich, G., Rajczak, J., Stoffel, M., 2014. 21st century climate change in the European Alps—a review. Sci. Total Environ. 493, 1138–1151. https://doi.org/10.1016/J.SCITOTENV.2013.07.050.
Groppelli, B., Bocchiola, D., Rosso, R., 2011a. Spatial downscaling of precipitation from GCMs for climate change projections using random cascades: a case study in Italy. Water Resour. Res. 47 https://doi.org/10.1029/2010WR009437.
Groppelli, B., Soncini, A., Bocchiola, D., Rosso, R., 2011b. Evaluation of future hydrological cycle under climate change scenarios in a mesoscale Alpine watershed of Italy. Nat. Hazard. Earth Syst. Sci. 11, 1769–1785. https://doi.org/10.5194/nhess-11-1769-2011.
Giudici, F., Anghileri, D., Castelletti, A., Burlando, P. 2020. Advancing the description of human decisions in catchment-scale hydrological models by including adaptive reservoir operations. J. Hydrol., under review.
GSE - Gestore Servizi Energetici, 2021. Sintesi rapporto delle attività 2020.
Haguma, D., Leconte, R., Côté, P., Krau, S., Brissette, F., 2014. Optimal hydropower generation under climate change conditions for a Northern Water Resources System. Water Resour. Manag. 28, 4631–4644. https://doi.org/10.1007/S11269-014-0763-3 (2014 2813 28).
Hazeleger, W., Wang, X., Severijns, C., Ştefănescu, S., Bintanja, R., Sterl, A., Wyser, K., Semmler, T., Yang, S., van den Hurk, B., van Noije, T., van der Linden, E., van der Wiel, K., 2012. EC-Earth V2.2: description and validation of a new seamless earth system prediction model. Clim. Dyn. https://doi.org/10.1007/s00382-011-1228-5.
Herman, J.D., Quinn, J.D., Steinschneider, S., Giuliani, M., Fletcher, S., 2020. Climate adaptation as a control problem: review and perspectives on dynamic water resources planning under uncertainty. Water Resour. Res. 56, e24389 https://doi.org/10.1029/2019WR025502.
Kasprzyk, J.R., Nataraj, S., Reed, P.M., Lempert, R.J., 2013. Many objective robust decision making for complex environmental systems undergoing change. Environ. Model. Softw. 42, 55–71. https://doi.org/10.1016/j.envsoft.2012.12.007.
Krysanova, V., Hattermann, F.F., Kundzewicz, Z.W., 2020. How evaluation of hydrological models influences results of climate impact assessment—an editorial. Clim. Change 163. https://doi.org/10.1007/s10584-020-02927-8.
Li, Y., 2016. Advancing coupled human-water systems analysis by agent-based modeling. Italy.
Manning, L.J., Hall, J.W., Fowler, H.J., Kilsby, C.G., Tebaldi, C., 2009. Using probabilistic climate change information from a multimodel ensemble for water resources assessment. Water Resour. Res. 45. https://doi.org/10.1029/2007WR006674.
Mastrotheodoros, T., Pappas, C., Molnar, P., Burlando, P., Manoli, G., Parajka, J., Rigon, R., Szeles, B., Bottazzi, M., Hadjidoukas, P., Fatichi, S., 2020. More green and less blue water in the Alps during warmer summers. Nat. Clim. Chang. 102 (10), 155–161. https://doi.org/10.1038/s41558-019-0676-5.
Mauritsen, T., Bader, J., Becker, T., Behrens, J., Bittner, M., Brokopf, R., Brovkin, V., Claussen, M., Crueger, T., Esch, M., Fast, I., Fiedler, S., Fläschner, D., Gayler, V., Giorgetta, M., Goll, D.S., Haak, H., Hagemann, S., Hedemann, C., Hohenegger, C., Ilyina, T., Jahns, T., Jimenéz-de-la-Cuesta, D., Jungclaus, J., Kleinen, T., Kloster, S., Kracher, D., Kinne, S., Kleberg, D., Lasslop, G., Kornblueh, L., Marotzke, J., Matei, D., Meraner, K., Mikolajewicz, U., Modali, K., Möbis, B., Müller, W. A., Nabel, J.E.M.S., Nam, C.C.W., Notz, D., Nyawira, S.S., Paulsen, H., Peters, K., Pincus, R., Pohlmann, H., Pongratz, J., Popp, M., Raddatz, T.J., Rast, S., Redler, R., Reick, C.H., Rohrschneider, T., Schemann, V., Schmidt, H., Schnur, R., Schulzweida, U., Six, K.D., Stein, L., Stemmler, I., Stevens, B., von Storch, J.S., Tian, F., Voigt, A., Vrese, P., Wieners, K.H., Wilkenskjeld, S., Winkler, A., Roeckner, E., 2019. Developments in the MPI-M earth system model version 1.2 (MPI-ESM1.2) and its response to increasing $CO_2$. J. Adv. Model. Earth Syst. 11, 998–1038. https://doi.org/10.1029/2018MS001400.
Peel, M.C., Finlayson, B.L., McMahon, T.A., 2007. Updated world map of the Köppen-Geiger climate classification. Hydrol. Earth Syst. Sci. 11, 1633–1644. https://doi.org/10.5194/hess-11-1633-2007.
Pellicciotti, F., Brock, B., Strasser, U., Burlando, P., Funk, M., Corripio, J., 2005. An enhanced temperature-index glacier melt model including the shortwave radiation balance: development and testing for Haut Glacier d'Arolla, Switzerland. J. Glaciol. 51, 573–587. https://doi.org/10.3189/172756505781829124.
Prudhomme, C., Wilby, R.L., Crooks, S., Kay, A.L., Reynard, N.S., 2010. Scenario-neutral approach to climate change impact studies: application to flood risk. J. Hydrol. 390, 198–209. https://doi.org/10.1016/j.jhydrol.2010.06.043.
Quinn, J.D., Reed, P.M., Giuliani, M., Castelletti, A., Oyler, J.W., Nicholas, R.E., 2018. Exploring how changing monsoonal dynamics and human pressures challenge multireservoir management for flood protection, hydropower production, and agricultural water supply. Water Resour. Res. 54, 4638–4662. https://doi.org/10.1029/2018WR022743.
Soncini, A., Bocchiola, D., Azzoni, R.S., Diolaiuti, G., 2017. A methodology for monitoring and modeling of high altitude Alpine catchments. Prog. Phys. Geogr. 41, 393–420. https://doi.org/10.1177/0309133317710832.
Stevens, B., Giorgetta, M., Esch, M., Mauritsen, T., Crueger, T., Rast, S., Salzmann, M., Schmidt, H., Bader, J., Block, K., Brokopf, R., Fast, I., Kinne, S., Kornblueh, L., Lohmann, U., Pincus, R., Reichler, T., Roeckner, E., 2013. Atmospheric component of the MPI-M earth system model: ECHAM6. J. Adv. Model. Earth Syst. 5, 146–172. https://doi.org/10.1002/jame.20015.
Wiley, M.W., Palmer, R.N., 2008. Estimating the impacts and uncertainty of climate change on a municipal water supply system. J. Water Resour. Plan. Manag. 134, 239–246. https://doi.org/10.1061/(ASCE)0733-9496(2008)134:3(239).
Zullo, F., Fazio, G., Romano, B., Marucci, A., Fiorini, L., 2019. Effects of urban growth spatial pattern (UGSP) on the land surface temperature (LST): a study in the Po Valley (Italy). Sci. Total Environ. 650, 1740–1751. https://doi.org/10.1016/J.SCITOTENV.2018.09.331.